Morris, J.D., Villinger, H.W., and Klaus, A. (Eds.)
Proceedings of the Ocean Drilling Program, Scientific Results Volume 205

4. Data Report: Carbon and Oxygen Isotope Geochemistry along a Subducting Pelagic Section Offshore Costa Rica (ODP Legs 170 and 205)[1]

Michael Strasser,[2] Helmut Weissert,[2] and Stefano M. Bernasconi[2]

ABSTRACT

In this data report we present results from stable isotope measurements ($\delta^{13}C$ and $\delta^{18}O$) on bulk sediment at several sites located on a transect along a subduction margin offshore Costa Rica (Ocean Drilling Program Sites 1039, 1040, and 1253). Comparison of stable isotope compositions ($\delta^{13}C$ and $\delta^{18}O$) of the pelagic carbonates Subunit U3C between the reference sites (Site 1039 and 1253) and the underthrust section (Site 1040) reveals similar $\delta^{13}C$ values and minor differences in $\delta^{18}O$ values within four specific intervals. Isotope stratigraphy was then used to further constrain the shipboard age models based on bio- and magnetostratigraphy. The resulting age models are in agreement with those derived from biostratigraphy and confirm that the sedimentation rate of the lower Subunit 3C is roughly constant on the order of 50 m/m.y. This is in contrast with the postulated very high sedimentation rates at ~12.7 Ma and lower sedimentation rates (~18 m/m.y.) in the lower part of the section between 16 and 13 Ma, as suggested by shipboard magnetostratigraphic datums.

[1] Strasser, M., Weissert, H., and Bernasconi, S.M., 2006. Data report: Carbon and oxygen isotope geochemistry along a subducting pelagic section offshore Costa Rica (ODP Legs 170 and 205). *In* Morris, J.D., Villinger, H.W., and Klaus, A. (Eds.), *Proc. ODP, Sci. Results,* 205, 1–18 [Online]. Available from World Wide Web: <http://www-odp.tamu.edu/publications/205_SR/VOLUME/CHAPTERS/205.PDF>. [Cited YYYY-MM-DD]
[2] Geological Institute, ETH Zurich, Universitaetsstrasse 16, CHN H71, CH-8092 Zurich, Switzerland.
Correspondence author: **strasser@erdw.ethz.ch**

Initial receipt: 28 February 2005
Acceptance: 22 November 2005
Web publication: 3 April 2006
Ms 205SR-205

INTRODUCTION

The Cocos plate offshore Costa Rica comprises igneous oceanic crust covered by 450 to 500 m of pelagic deposits. Along the Costa Rica convergent margin, this plate is being subducted beneath a prism wedge attached to the Caribbean plate (Morris, Villinger, Klaus, et al., 2003, and references therein) (Figs. F1, F2). During Ocean Drilling Program (ODP) Legs 170 and 205, the sedimentary succession of the subducting plate was drilled at reference sites oceanward of the deformation front (Sites 1039 and 1253) and was also recovered at a prism site (Site 1040) below the décollement (Fig. F2).

At reference Site 1039, three sedimentary units and one intrusive unit were recovered (Kimura, Silver, Blum, et al., 1997) (Fig. F3). Unit U1 consists of dark olive-green diatomaceous ooze intercalated with ash layers. Below a sharp contact, Unit U2 is distinguished by a rapid decrease in biogenic sediment and consists of dark olive-green silty clay interbedded with light olive-green calcareous clay and ash layers. Unit U3 exhibits a dramatic increase in biogenic sedimentation, changing sharply from the nearly barren clays of Unit U2 to ivory to light green and mottled siliceous calcareous oozes interbedded with calcareous clay and ash. The basal oozes of Subunit U3C are metaliferous. The igneous Unit U4 consists of fine-grained gabbros that are interpreted as intrusive sill (Kimura, Silver, Blum, et al., 1997). Below this ~35-m-thick igneous unit, another ~20 m of pelagic sediment (Subunit U3C) was recovered during Leg 205 at Site 1253 (Morris, Villinger, Klaus, et al., 2003).

Drilling at Sites 1040 and 1043 and subsequent studies (Morris, Villinger, Klaus, et al., 2003, and references therein) show that the sediment section beneath the décollement repeats the complete lithology and sequence of the subducting plate cored at Site 1039 (Fig. F3). Also, the seismic observations indicate complete sediment subduction past the prism front (Fig. F2). The thinning of the underthrust section seen between Sites 1039 and 1040 (Figs. F2, F3) must then reflect compaction and dewatering processes. This leads to a change of the corresponding lithologies from silty clay and calcareous oozes at Sites 1039 and 1253 to claystones and calcareous chalk in the underthrust section at Site 1040.

The progressive subduction of the pelagic sediment section along the Costa Rica convergent margin offers the possibility to study in detail compaction and dewatering processes during early subduction. The signature of such processes should be seen in chemical proxies due to diagenesis and alteration of the pelagic sediments. By comparing the chemical signature in the sediments at the reference sites with those of the underthrust section, effects of compaction and dewatering processes on diagenesis could be estimated. In this data report, we present results on stable isotope compositions that show significant differences in the $\delta^{18}O$ values between the unaffected carbonates in sedimentary Unit U3 at reference Sites 1039 and 1253 and the equivalent underthrust section at Site 1040. These results could be used in further studies to test models of sediment compaction and dewatering processes during early subduction.

In addition, the stable isotope analyses of the pelagic carbonates in the reference site oceanward of the deformation front (Site 1039) are used as a chemostratigraphic tool to complement the bio- and magnetostratigraphy of the carbonate section (Kimura, Silver, Blum, et al.,

F1. Leg 170 and 205 drilling areas, p. 7.

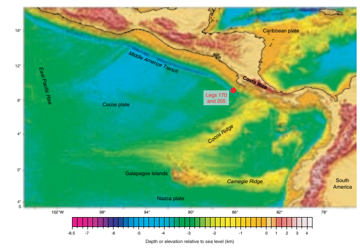

F2. Seismic profile, p. 8.

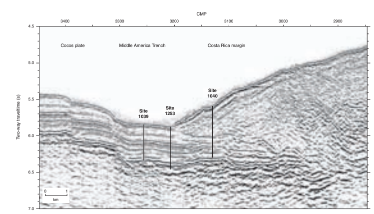

F3. Recovered lithologies, p. 9.

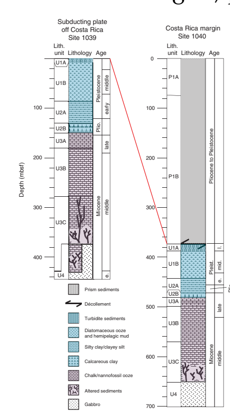

1997; Muza, 2000). The occurrence of positive shifts in carbonate $\delta^{13}C$ values of up to 1.5‰ in the middle Miocene (known as the Monterrey excursion, between 13 and ~17.5 Ma) has been described by Vincent and Berger (1985) in a data set from Deep Sea Drilling Project (DSDP) Site 216 in the tropical Indian Ocean and correlated to several stratigraphic sections all over the world (Woodruff and Savin, 1991; Jacobs et al., 1996; John et al., 2003). The Monterey excursion comprises several higher frequency (~400 k.y. cycles) peaks (carbon isotope maxima [CM]) (Woodruff and Savin, 1991), presumably caused by orbital climate forcing corresponding to long eccentricity cycles (Cramer et al., 2003). Reproducing these isotopic peaks in the analyzed samples from ODP Leg 170 leads to an isotope stratigraphy that is supportive of the biostratigraphy established by Muza (2000), especially in the range between 270 and 370 meters below seafloor (mbsf) (Site 1039), where biostratigraphic datums are lacking and magnetostratigraphic datums reveal controversial ages.

METHODS

For isotopic analyses, 5-cm^3 samples from the carbonate-rich interval in Hole 1039B (Cores 170-1039B-21X through 41X) were examined at a ~10- (in Subunit U3B) to 5-m (in Subunit U3C) resolution. The same sample volumes were analyzed every ~8 (in Subunit U3B) to 4 m (in Subunit U3C) from the corresponding cores in Hole 1040C (Cores 170-1040C-36R through 52R). In addition to samples from Leg 170, a few samples from the lowermost interval of Subunit U3C recovered during Leg 205 were examined (5-cm^3 samples from squeeze cake material from Cores 205-1253A-1R through 4R and 10-R through 12R; freeze dried at –80°C).

The oxygen and carbon isotope analyses of bulk sediment samples were conducted on a VG Isotech Prism Series II isotope ratio mass spectrometer fitted with a common acid bath automated carbonate device. Clean bulk samples (without pretreatment) were reacted in orthophosphoric acid maintained at 90°C by a water bath and cryogenically purified from water and noncondensable gases before introduction into the mass spectrometer. Analytical reproducibility is better than ±0.1‰ for $\delta^{13}C$ and $\delta^{18}O$ values and was monitored through multiple analyses of a laboratory standard, which has been calibrated to the isotopic reference material National Bureau of Standards (NBS)-18 and NBS-19 for conversion to Vienna Peedee belemnite (VPDB) scale. Carbon and oxygen isotope ratios are reported in the conventional delta notation relative to the Vienna Peedee belemnite standard.

Sediment horizon correlations were used to compare the isotopic signals from Site 1039 with the signals from Site 1040. These were established by calculating the solid height profiles (i.e., the theoretical depth profile in a decompacted sedimentary section of solid material only, calculated from measured porosities data) at each site and by assuming constant accumulation rates (D. Saffer, pers. comm., 2002). The sediment horizon correlations are consistent with the boundaries between lithologic units and allow transforming Site 1040 depths to corresponding depths in the reference Site 1039. The transformation is depth dependent and has an estimated maximal absolute error of ~3.5 m.

To construct the age model, the results from Site 1039 were compared visually with the published isotope data from Woodruff and Savin (1991) and John et al. (2003). Maximum ($\delta^{13}C$) and minimum

($\delta^{18}O$) peaks in the measured data were matched to CM 1–6 and $\delta^{18}O$ Events A–F, respectively (Woodruff and Savin, 1991).

RESULTS

Stable Isotope Geochemistry

Results from stable isotope measurements are displayed in Table T1 and shown in Figure F4. The isotopic composition of bulk sediment samples from the carbonate section (Subunits U3B and U3C) falls between –1‰ and +1‰ for $\delta^{18}O$ and between 1.5‰ and 3‰ for $\delta^{13}C$. Only in the immediate vicinity of the intrusive gabbroic unit (U4) are values clearly more negative, reaching values as low as –20.5‰ $\delta^{18}O$ and –0.4‰ $\delta^{13}C$. This negative shift is interpreted as the result of thermal alteration caused by gabbro emplacement and is not further considered in this study.

A comparison of isotope data from the pelagic sections at Sites 1039 and 1040 (Fig. F5) reveals that $\delta^{13}C$ values from both sites are virtually indistinguishable, except for the interval between 310 and 330 mbsf in the composite section where the two sites show slightly different $\delta^{13}C$ values outside analytical error. On the other hand, $\delta^{18}O$ values of bulk sediment samples from Site 1039 are more negative in four specific intervals (marked with yellow bars in Fig. F5) but do not show significant differences in the other part of the section. A maximum deviation of ~0.75‰ in $\delta^{18}O$ that clearly lies above the measurement and depth transformation error is reached in the lowermost 30 m of Subunit U3C immediately above the gabbro sill.

From available data at Site 1040, there is no evidence for higher porosity or for significant lithologic or composition differences that would indicate possible fluid flow or local diagenetic alteration in the respective intervals. However, the observed interval-specific offsets in the oxygen isotopic signal between the reference site and the underthrusted section are significant and need further study to investigate their implications for diagenetic alteration and fluid flow during early subduction.

Isotope Stratigraphy and Age Model

With the assumption that general trends in bulk sediment isotopic composition at the reference Site 1039 mainly reflect trends in the primary isotopic composition of the pelagic carbonaceous components (i.e., coccolithophorids and foraminifers that are well preserved in smear slides and visually do not show diagenetic imprinting; Morris, Villinger, Klaus, et al., 2003; Kimura, Silver, Blum, et al., 1997), results from stable isotope geochemistry are used to establish an isotope stratigraphy for the studied section. Data from $\delta^{13}C$ analyses show dominant positive peaks of up to 1.5‰ (e.g., at 260 mbsf at Site 1039) that can be correlated to CM events of the Monterey excursion in the middle Miocene (Woodruff and Savin, 1991). Figure F6 shows the correlation between the maximum $\delta^{13}C$ peaks in Unit U3 of Site 1039 and CM 1–6 measured in a pelagic section in DSDP Site 574 from the equatorial Pacific (Woodruff and Savin, 1991) and outcrop data from a section on the Maltese Islands (John et al., 2003). Site 574 was further used to correlate minima in $\delta^{18}O$ values ($\delta^{18}O$ Events A–F; Woodruff and Savin, 1991), revealing a robust age control on the lower stratigraphic section of Site 1039 (Figs. F6, F7).

T1. Isotope values, p. 17.

F4. Isotope values, p. 10.

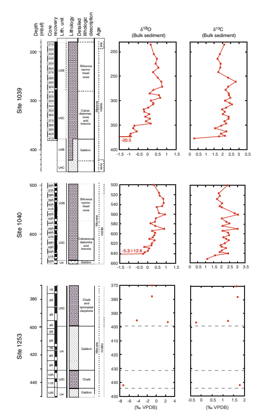

F5. Isotope compositions, p. 11.

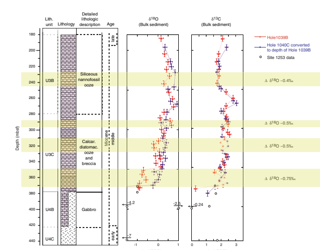

F6. Carbon isotope values, p. 13.

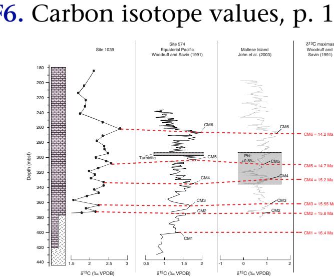

F7. Oxygen isotope values, p. 15.

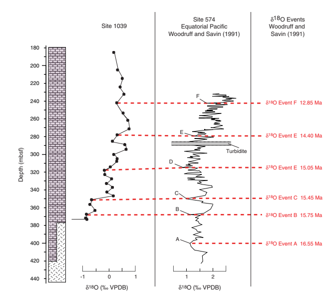

The absolute chronology of the middle Miocene carbonate section recovered at Site 1039 is shown as an age vs. depth diagram in Figure F8. It is compiled from all available biostratigraphic, magnetostratigraphic, and isotopic datums (Kimura, Silver, Blum, et al., 1997; Muza, 2000) (Table T2). The stable isotope stratigraphy presented here is in agreement with the age models derived from biostratigraphy (Muza, 2000) and confirms that sedimentation rate of the middle Miocene carbonate-rich Subunits U3B and U3C is constant and on the order of 50 m/m.y. This is in contrast with the very high sedimentation rates at ~12.7 Ma and lower sedimentation rates (~18 m/m.y.) in the lower part of the section between 16 and 13 Ma, as inferred from the magnetostratigraphic datums (Kimura, Silver, Blum, et al., 1997).

F8. Age-depth diagram, p. 16.

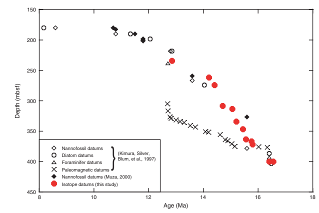

T2. Compiled datums, p. 18.

ACKNOWLEDGMENTS

We would like to thank Maria Coray for assistance with the mass spectrometer and Cédric John for helpful comments on a previous version of the manuscript. I am grateful to the Leg 205 Shipboard Party for their assistance and to the Co-Chief Scientists, who offered me as a Student Trainee the opportunity to work as a sedimentologist on board the *JOIDES Resolution* and thus to realize the study presented here.

This research used samples and data provided by the Ocean Drilling Program (ODP). ODP is sponsored by the U.S. National Science Foundation (NSF) and participating countries under management of Joint Oceanographic Institutions (JOI), Inc. This research was supported by ETH Zurich and the Swiss National Fund (SNF).

REFERENCES

Cramer, B.S., Wright, J.D., Kent, D.V., and Aubry, M., 2003. Orbital forcing of $\delta^{13}C$ exursions in the late Paleocene–early Eocene (Chrons C24n–C25n). *Palaeogeography,* 18(4):1097.

Jacobs, E., Weisser, H., Shields, G., and Stille, P., 1996. The Monterey event in the Mediterranean: a record from shelf sediments of Malta. *Paleoceanography,* 11(6):717–728. **doi:10.1029/96PA02230**

John, C.M., Mutti, M., and Adatte, T., 2003. Mixed carbonate-siliciclastic record on the North African margin (Malta)—coupling of weathering processes and mid-Miocene climate. *Bull. Geol. Soc. Am.,* 115(2):217–229.

Kimura, G., Silver, E.A., Blum, P., et al., 1997. *Proc. ODP, Init. Repts.,* 170: College Station, TX (Ocean Drilling Program). [**HTML**]

Morris, J.D., Villinger, H.W., Klaus, A., et al., 2003. *Proc. ODP, Init. Repts.,* 205 [Online]. Available from World Wide Web: <http://www-odp.tamu.edu/publications/205_IR/205ir.htm>. [Cited 2005-02-21]

Muza, J.P., 2000. Calcareous nannofossil biostratigraphy from a 15-km transect (Cocos plate to Caribbean plate) across the Middle America Trench, Nicoya Peninsula, Costa Rica. *In* Silver, E.A., Kimura, G., Blum, P., and Shipley, T.H. (Eds.), *Proc. ODP, Sci. Results,* 170 [Online]. Available from World Wide Web: <http://www-odp.tamu.edu/publications/170_SR/chap_05/chap_05.htm>. [Cited 2005-02-21]

Smith, W.H.F., and Sandwell, D.T., 1997. Global seafloor topography from satellite altimetry and ship depth soundings. *Science,* 277:1956–1962. **doi:10.1126/science.277.5334.1956**

Vannucchi, P., Ranero, C.R., Galeotti, S., Straub, S.M., Scholl, D.W., and McDougall-Ried, K., 2003. Fast rates of subduction erosion along the Costa Rica Pacific margin: implications for nonsteady rates of crustal recycling at subduction zones. *J. Geophys. Res.*, 108(B11):2511. **doi:10.1029/2002JB002207**

Vincent, E., and Berger, W.H., 1985. Carbon dioxide and polar cooling in the Miocene: the Monterey Hypothesis. *In* Sundquist, E.T., and Broecker, W.S. (Eds.), *The Carbon Cycle and Atmospheric* CO_2*: Natural Variations Archean to Present.* Geophys. Monogr., 32:455–468.

Woodruff, F., and Savin, S.M., 1991. Mid-Miocene isotope stratigraphy in the deep-sea: high resolution correlations, paleoclimatic cycles, and sediment preservation. *Paleoceanography,* 6:755–806.

Figure F1. Bathymetric map of the eastern central Pacific showing Leg 170 and 205 drilling areas in the Middle America Trench offshore Costa Rica. Map is modified after Vannucchi et al. (2003). Elevation data are from Smith and Sandwell (1997).

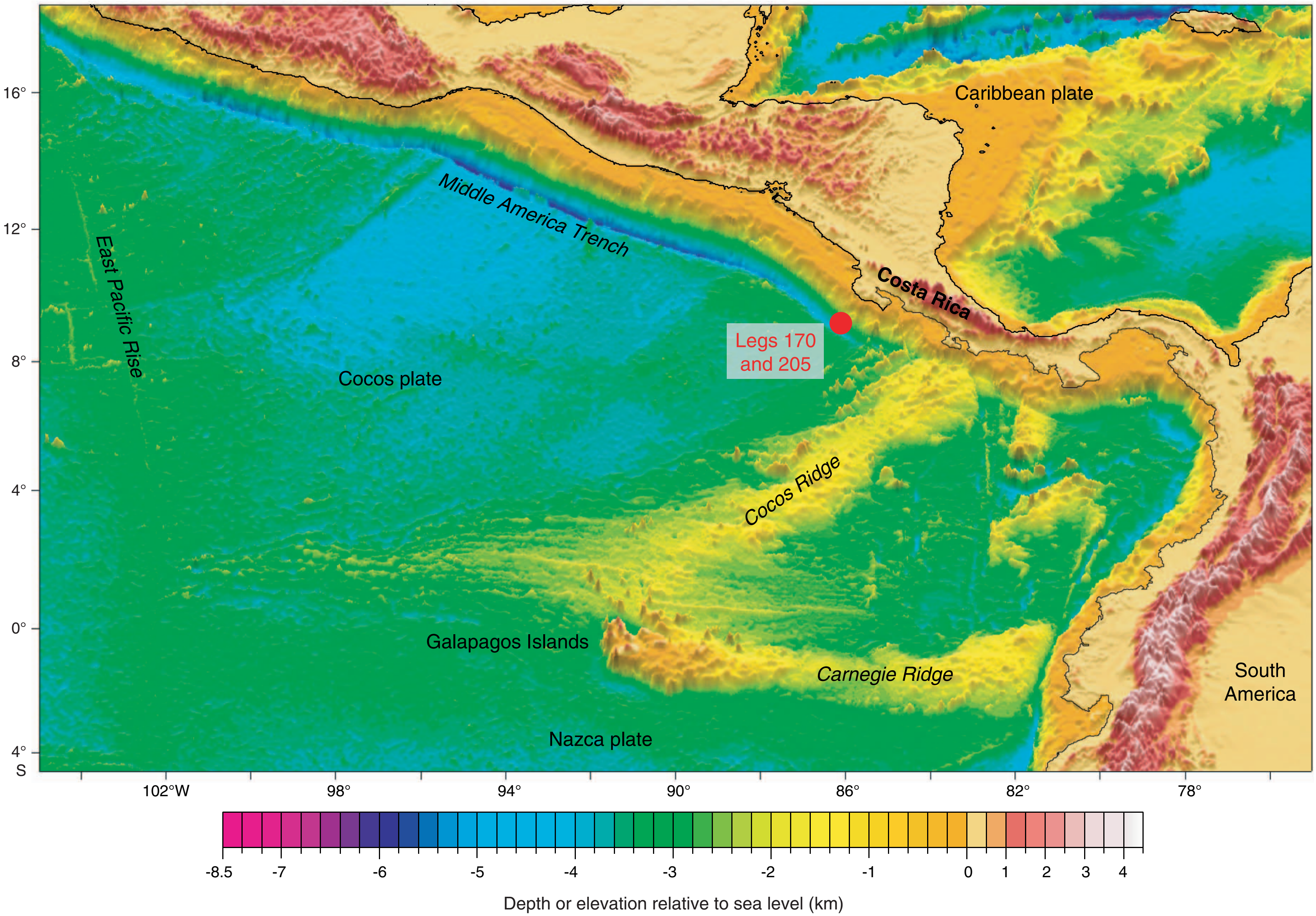

Figure F2. Migrated multichannel seismic Profile BGR-99-44 (C. Ranero and C. Reichert, pers. comm., 2001) across the Middle America Trench showing the general structure of the seaward side of the Middle America Trench, the trench itself, and the lowermost seaward part of the prism. CMP = common midpoint. Shot point numbers from multichannel seismic survey.

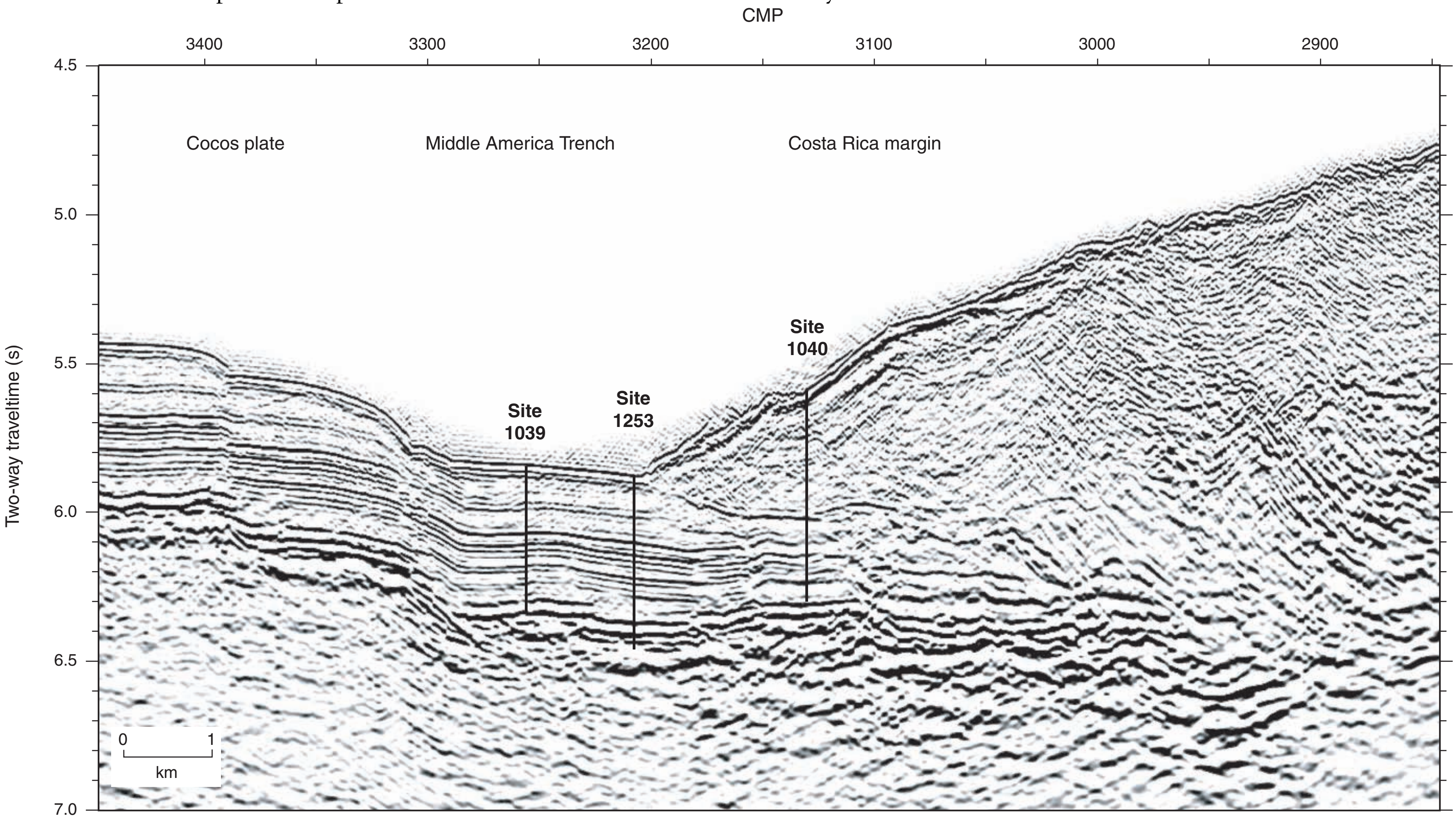

Figure F3. Summary showing recovered lithologies drilled on the incoming plate (Site 1039) and on the Costa Rica margin (Site 1040) (modified after Kimura, Silver, Blum, et al., 1997). Note the repetition of the Site 1039 section below the décollement at Site 1040.

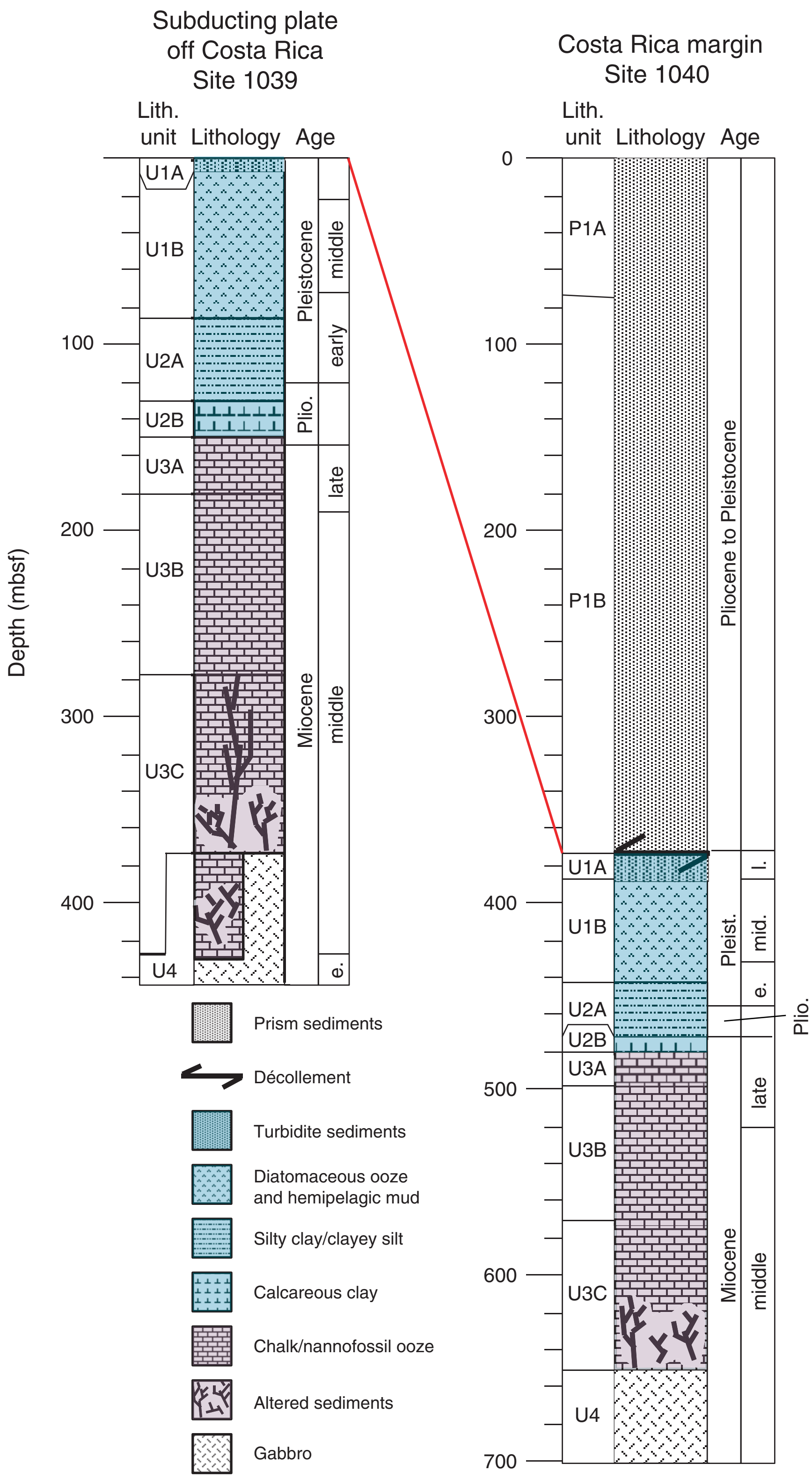

Figure F4. Composite showing lithologic units and bulk sediment δ^{18}O and δ^{13}C values from Sites 1039, 1040, and 1253. Negative δ^{18}O values close to the contact with the gabbro sill that plotted outside the range are given in numbers. Note change in depth scale between diagrams. See Figure F3, p. 9, for lithology keys. VPDB = Vienna Peedee belemnite.

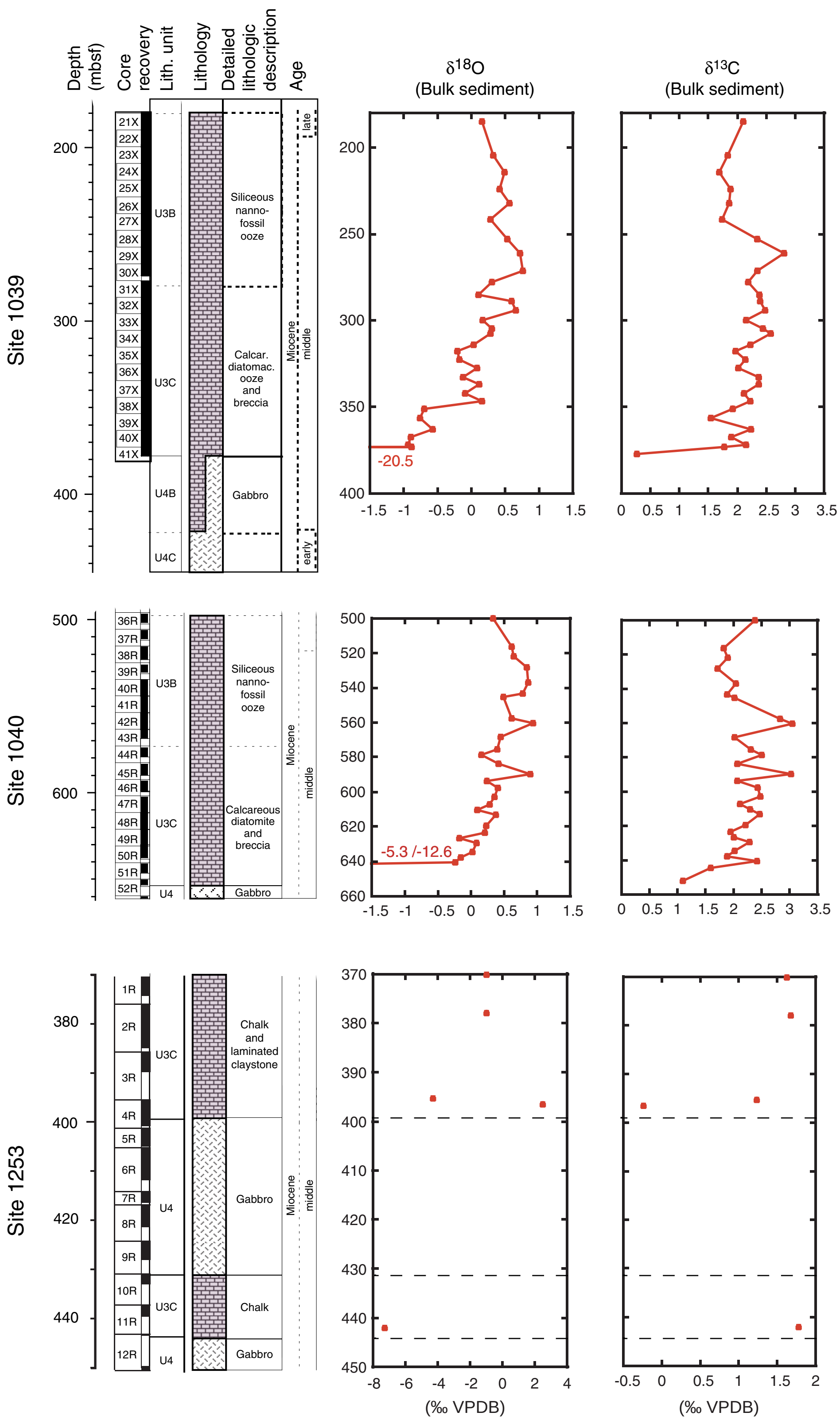

Figure F5. Comparison of carbon and oxygen isotope compositions between reference Site 1039 and underthrust section at Site 1040. Transformation from Site 1040 depth to the corresponding depth in reference Site 1039 is based on the sediment horizon correlations that were established by calculating the solid height profiles (i.e., the theoretical depth profile in a decompacted sedimentary section of solid material only, calculated from measured porosity data) at each site and by assuming constant accumulation rates (D. Saffer, pers. comm., 2002). Also shown are data points from Site 1253 which are projected into the depth of Site 1039. Error bars show precision of isotope measurements (±0.1‰) and error of depth transformation (3.5 m). Yellow bars indicate four specific intervals where $\delta^{18}O$ values vary significantly between the reference and underthrust site. VPDB = Vienna Peedee belemnite. (**Figure shown on next page.**)

Figure F5 (continued). (Caption shown on previous page.)

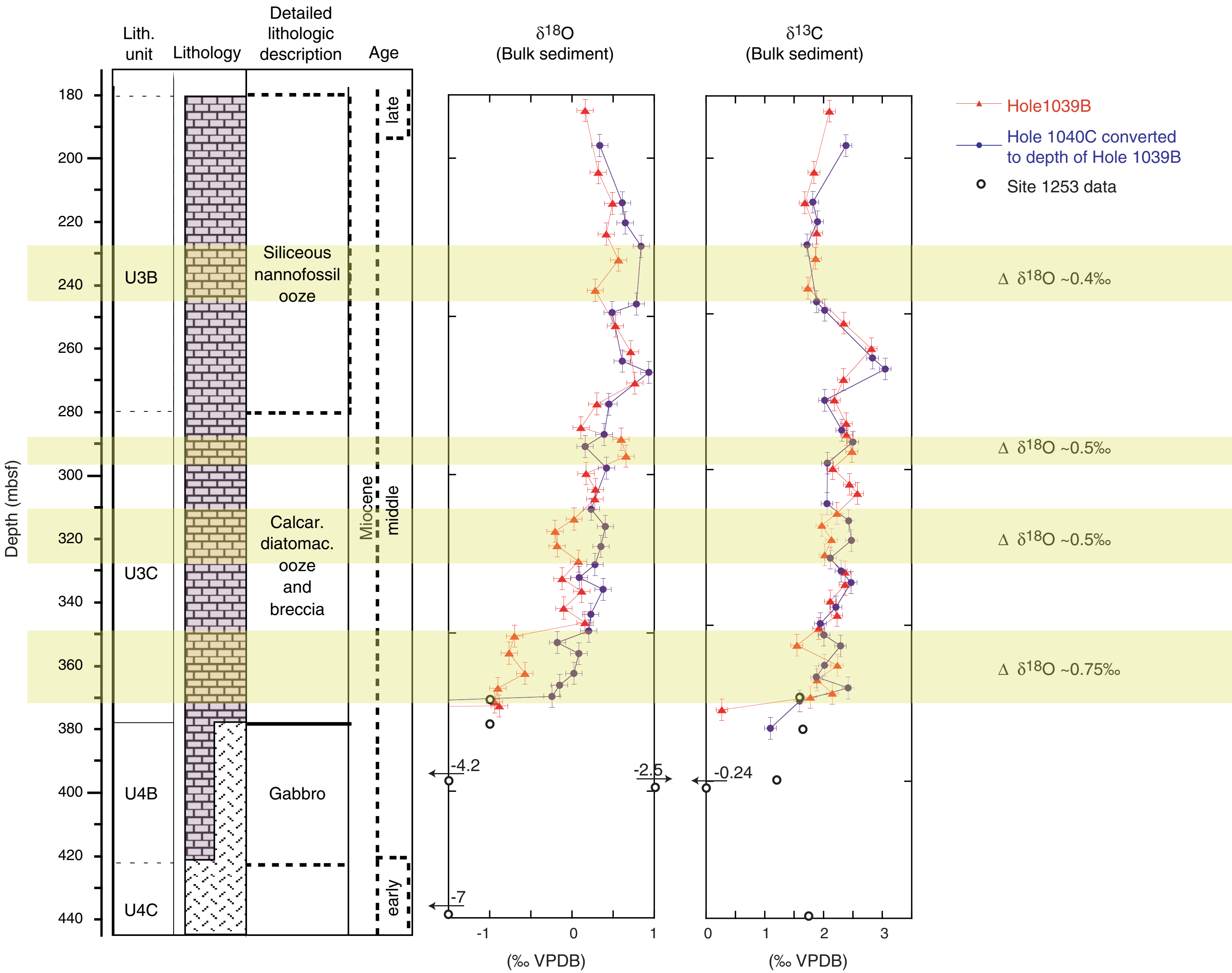

Figure F6. Bulk sediment $\delta^{13}C$ values from Site 1039 correlated to middle Miocene $\delta^{13}C$ records from a pelagic section at Site 574 in the equatorial Pacific (Woodruff and Savin, 1991) and from outcrop data on the Maltese Islands (John et al., 2003). Maximum peaks were matched to carbon isotope maximums (CM) 1–6 (Woodruff and Savin, 1991). Note that absolute values between the three sites are not compared because of lithologic differences, but relative trends and amplitudes of positive $\delta^{13}C$ excursions are used instead to allow for a robust correlation. Intervals marked with gray bars show specific lithologic intervals that contrast with the general stratigraphic column. In order to use a common scale, $\delta^{13}C$ values from the phosphatic layer (Phl) in the Maltese section are shifted 0.8‰ toward more positive values. VPDB = Vienna Peedee belemnite. (**Figure shown on next page.**)

Figure F6 (continued). (Caption shown on previous page.)

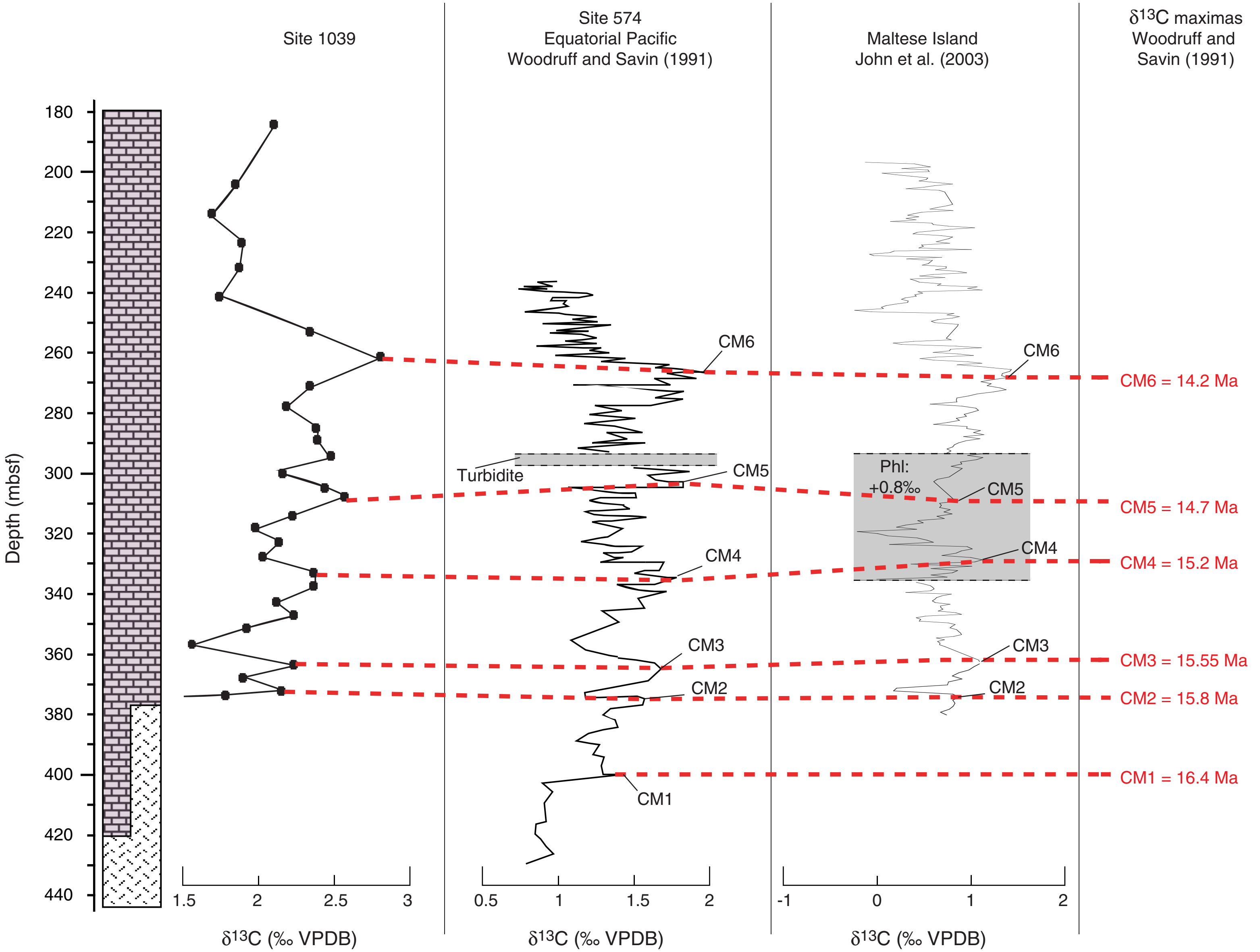

Figure F7. Bulk sediment δ^{18}O values from Site 1039 correlated to middle Miocene δ^{18}O records from pelagic section at equatorial Pacific Site 574 (Woodruff and Savin, 1991). Minimum troughs were matched to δ^{18}O Events A–F (Woodruff and Savin, 1991). Note that the absolute values are not comparable between the two sites because of lithologic differences, but relative trends and the amplitudes of negative δ^{18}O excursions allow for a robust correlation. VPDB = Vienna Peedee belemnite.

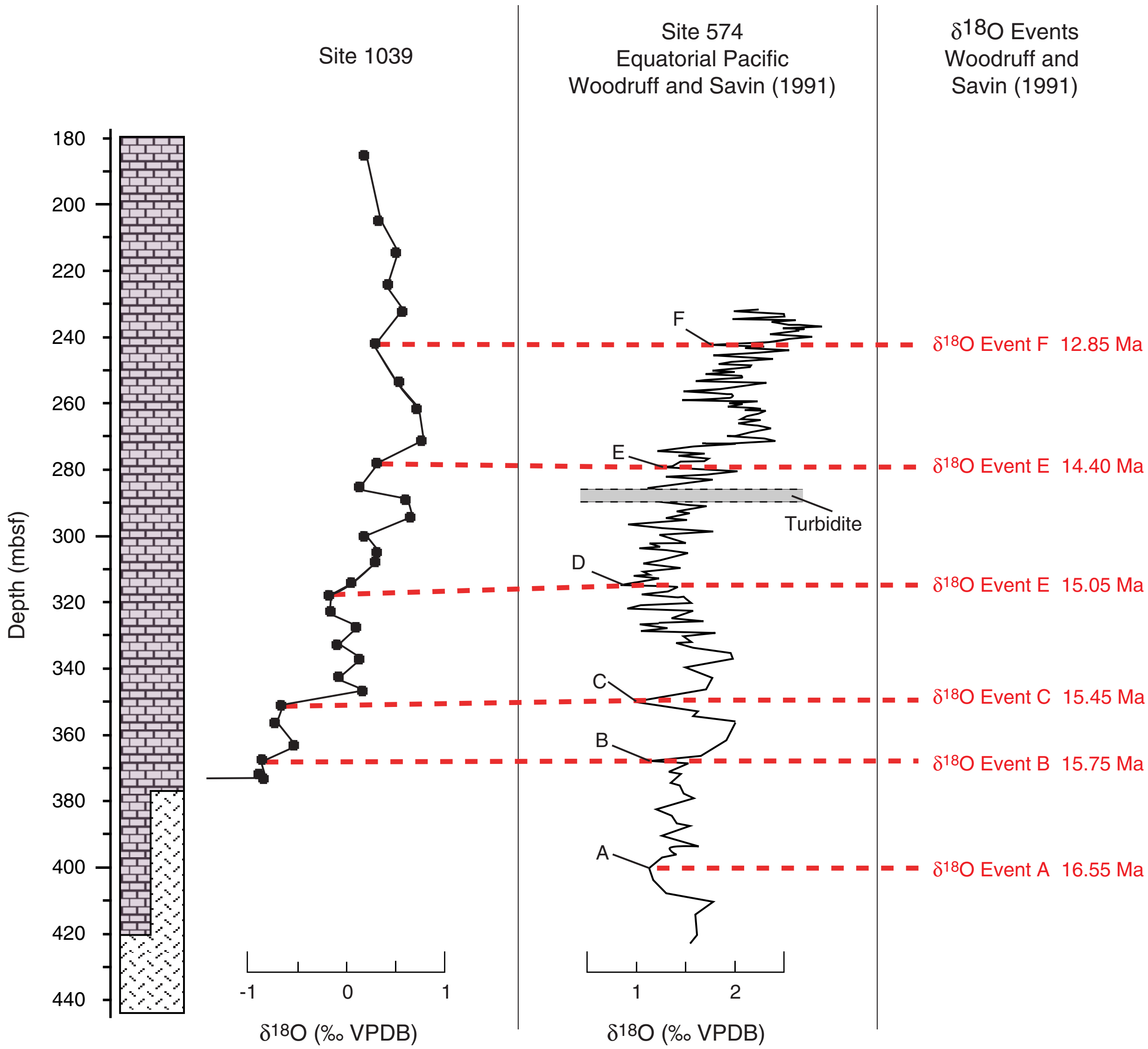

Figure F8. Age-depth diagram for middle Miocene carbonate section at Site 1039 compiled from all available biostratigraphic, magnetostratigraphic, and isotopic datums.

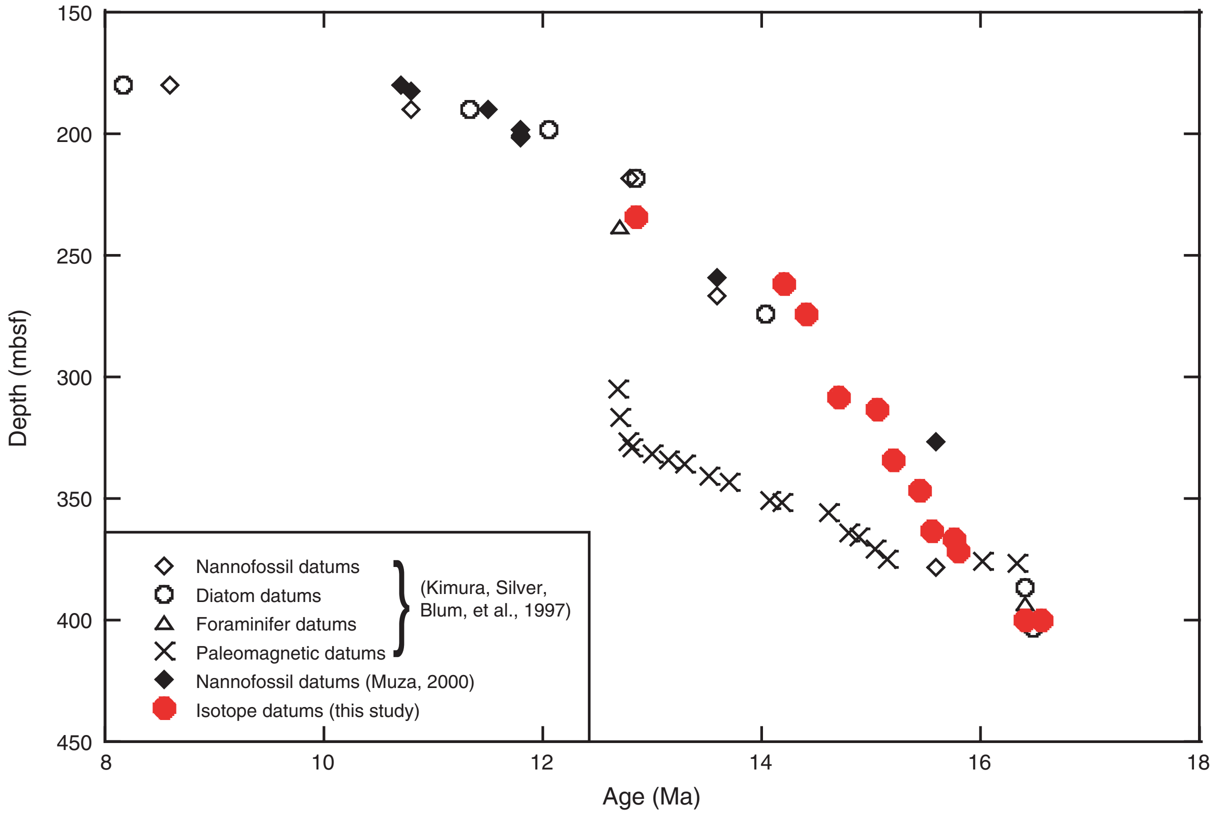

Table T1. $\delta^{18}O$ and $\delta^{13}C$ values of bulk sediment samples, Sites 1039, 1040, and 1253.

Core, section, interval (cm)	Depth (mbsf)	$\delta^{18}O$ (‰ VPDB)	$\delta^{13}C$ (‰ VPDB)
170-1039B-			
21X-4, 25–26	184.95	0.160	2.102
23X-4, 55–56	204.55	0.321	1.840
24X-4, 75–76	214.35	0.495	1.685
25X-4, 85–86	224.05	0.419	1.886
26X-3, 80–81	232.20	0.567	1.864
27X-3, 75–76	241.75	0.284	1.733
28X-4, 80–81	253.00	0.529	2.344
29X-3, 80–81	261.20	0.715	2.813
30X-3, 100–101	271.10	0.765	2.341
31X-1, 100–101	277.70	0.304	2.187
31X-6, 100–101	285.20	0.110	2.386
32X-2, 95–96	288.85	0.599	2.393
32X-6, 30–31	294.20	0.659	2.483
33X-3, 70–71	299.70	0.172	2.158
33X-6, 120–121	304.70	0.299	2.442
34X-2, 57–58	307.67	0.278	2.577
34X-6, 95–96	314.05	0.027	2.229
35X-2, 120–121	317.90	–0.204	1.973
35X-5, 130–131	322.50	–0.179	2.136
36X-2, 105–106	327.35	0.081	2.022
36X-6, 60–61	332.90	–0.120	2.366
37X-2, 100–101	336.90	0.119	2.366
37X-6, 30–31	342.20	–0.098	2.115
38X-2, 130–131	346.80	0.158	2.230
38X-5, 100–101	351.00	–0.697	1.916
39X-2, 130–131	356.40	–0.762	1.547
39X-7, 20–21	362.80	–0.5714	2.236
40X-3, 130–131	367.50	–0.8994	1.891
40X-6, 110–111	371.80	–0.9384	2.149
41X-1, 30–31	373.10	–0.8824	1.778
41X-3, 130–131	377.10	–19.818	0.271
170-1040C-			
36R-3, 99–100	499.99	0.339	2.385
38R-1, 103–104	516.33	0.613	1.821
38R-5, 52–53	521.82	0.649	1.899
39R-3, 27–28	528.17	0.842	1.719
40R-2, 100–101	537.00	0.868	2.048
40R-6, 122–123	543.22	0.784	1.882
41R-1, 130–131	545.40	0.490	2.019
42R-3, 90–91	557.60	0.612	2.834
42R-5, 90–91	560.40	0.937	3.051
43R-4, 30–31	568.20	0.449	2.021
44R-2, 100–101	575.60	0.392	2.311
44R-4, 90–91	578.50	0.161	2.500
45R-1, 100–101	583.70	0.421	2.066
45R-5, 91–92	589.61	0.892	3.024
46R-1, 135–136	593.65	0.236	2.061
46R-4, 104–105	597.84	0.407	2.428
47R-1, 80–81	602.70	0.353	2.475
47R-4, 68–69	607.08	0.281	2.115
47R-6, 90–91	610.30	0.090	2.300
48R-2, 10–11	613.20	0.379	2.471
48R-6, 30–31	619.40	0.230	2.212
49R-2, 90–91	623.60	0.205	1.945
49R-4, 85–86	626.55	–0.177	2.008
49R-6, 70–71	629.40	0.085	2.291
50R-3, 76–77	634.56	0.025	2.018
50R-5, 88–89	637.68	–0.1504	1.879
51R-1, 31–32	640.71	–0.2414	2.419
51R-3, 95–97	644.35	–4.8968	1.595
52R-2, 65–66	652.15	–12.602	1.098
205-1253A-			
1R-1, 13–29	370.13	–0.96	1.624
2R-2, 85–104	377.95	–0.980	1.681
4R-1, 45–46	395.35	–4.289	1.231
4R-2, 15–16	396.55	2.503	–0.239
12R-1, 8–9	442.08	–7.270	1.777

Note: VPDB = Vienna Peedee belemnite.

Table T2. Compiled biostratigraphic, magnetostratigraphic, and isotopic datums, Site 1039.

Depth (mbsf)	Biostratigraphic datum Age (Ma)				Paleomagnetic datum* Age (Ma)	Isotopic datums Age (Ma)
	Nannofossil		Diatom*	Foraminifer*		
180.37	8.6*	10.7†	8.17			
182.21		10.8†				
189.87	10.8*		11.34			
189.87		11.5†				
198.65	11.8*		12.06	11.8		
198.65		11.8†				
201.51		11.8†				
218.43	12.8*		12.86			
234.5						12.85
238				12.7		
259.4		13.6†				
262						14.2
266.84	13.6*					
274						14.4
274.15			14.03			
305					12.678	
308						14.7
313						15.05
317					12.708	
326.83		15.6†				
327					12.775	
329					12.819	
332					12.991	
334					13.139	15.2
336					13.302	
341					13.51	
343					13.703	
347						15.45
351					14.076	
352					14.178	
356					14.612	
363						15.55
364					14.8	
366					14.888	
367						15.75
371					15.034	
372						15.8
375					15.155	
376					16.014	
377					16.327	
378.15	15.6*					
386.39			16.4			
393.6				16.4		
400						16.55
403.06			16.49			

Note: * = Kimura, Silver, Blum, et al. (1997), † = Muza (2000), ‡ = this study.